Available online at www.sciencedirect.com
ScienceDirect
Ceramics International 34 (2008) 797–801
CERAMICS INTERNATIONAL
www.elsevier.com/locate/ceramint

Ferroelectric and ferromagnetic properties of Mn-doped $0.7BiFeO_3$–$0.3BaTiO_3$ solid solution

Xiao-Hui Liu *, Zhuo Xu, Shao-Bo Qu, Xiao-Yong Wei, Jiang-Li Chen

Electronic Materials Research Laboratory, Key Laboratory of the Ministry of the Education, Xi'an Jiaotong University, Xi'an 710049, China

Available online 4 October 2007

Abstract

Binary solid solutions $0.7BiFeO_3$–$0.3BaTiO_3$–x wt.% MnO_2 ($x = 0$, 0.2, 0.3, and 0.5) were prepared by a traditional ceramic process. All ceramic samples show single perovskite phase. The effect of manganese doping on structure, dielectric, ferroelectric and ferromagnetic properties, and resistivity was investigated. Results show that Mn-dopant can improve the sintering ability of the materials when MnO_2 content is below 0.3 wt.%. When MnO_2 content exceeds 0.3 wt.%, the sintering ability is weakened and the phase structure of $0.7BiFeO_3$–$0.3BaTiO_3$ solid solution changes from rhombohedral into tetragonal phase. With increasing concentration of MnO_2, the resistivity increases at first and then decreases. Whereas the coercive electric field decreases at first and then increases, the remanent magnetization M_r increases and the coercive magnetic field decreases.

© 2007 Published by Elsevier Ltd and Techna Group S.r.l.

Keywords: Ferroelectricity; Ferromagnetism; $0.7BiFeO_3$–$0.3BaTiO_3$ solid solution

1. Introduction

Synthesis of ferroelectromagnetic material exhibiting ferromagnetism and ferroelectricity simultaneously has been an interesting subject, not only for possible applications in electronic devices, but also for the fundamental understanding of solid-state physics [1]. Most of single-phase ferroelectromagnetic materials have few applications due to their low Néel temperature or Curie temperature except some materials such as $BiFeO_3$. $BiFeO_3$ and its solid solutions have high Néel temperature and high Curie temperature. However, one of the major problems of earlier $BiFeO_3$-based materials is the low resistivity which has prevented practical application of the material as piezoelectric or magnetoelectric functional components. The relatively high conductivity of $BiFeO_3$ is believed to originate from the reduction of Fe^{3+} species to Fe^{2+}, creating oxygen vacancies for charge compensation [2]. At present, there are two ways used to solve the problem, one is to add perovskites (such as $PbTiO_3$, $BaTiO_3$, and $SrTiO_3$) [2–4] into solid solution with $BiFeO_3$ in order to stabilize a perovskite structure and enhance the electric insulation resistance, the other is to add some dopants such as gallium [2], neodymium, and tantalum [5,6] to improve properties. Although the perovskite structure of these solid solutions has been shown to be stable, to date the insulation resistance of $BiFeO_3$-based materials has not been raised sufficiently, and the ferroelectric and ferromagnetic properties of $BiFeO_3$-based solid solutions have not been improved greatly. Since manganese is a magnetic element with multiple valences, the present study is intended to improve properties of $BiFeO_3$-based materials by doping manganese, on which few reports have been found to date.

In this work, the focus is on the effect of Mn doping on the structure, dielectric, resistivity, ferroelectric and ferromagnetic properties of $0.7BiFeO_3$–$0.3BaTiO_3$ solid solution. Possible mechanisms have been discussed.

2. Experimental procedure

$0.7BiFeO_3$–$0.3BaTiO_3$–x wt.%MnO_2 solid solutions were fabricated by conventional solid-state reaction with $x = 0$, 0.2, 0.3, and 0.5, respectively. The starting materials used were Bi_2O_3, Fe_2O_3, $BaCO_3$, TiO_2, and MnO_2, which all had purities greater than 99%. The oxide powders were mixed in a ball mill for 12 h, using alcohol as media. After drying, the powders

---

* Corresponding author.
E-mail address: lxhui@mail.xjtu.edu.cn (X.-H. Liu).

0272-8842/$34.00 © 2007 Published by Elsevier Ltd and Techna Group S.r.l.
doi:10.1016/j.ceramint.2007.09.029

were calcined at 810 °C for 2 h in the air, and ball milling for another 12 h. The resultant powders with 5 wt.% polyvinyl alcohol as a binder were pressed as disks in a stainless steel die under a pressure of 400 MPa. After pressing, the disks were 10 mm in diameter and 1.2 mm in thickness, and sintered at 900–1000 °C for 2 h in the air.

The structure and phase evolution of specimens were characterized by X-ray diffraction (XRD) (Rigaku D/MAX-2400, Cu Kα radiation). The microstructure of fresh fracture surfaces of sintered pellets was examined by scanning electron microscopy (SEM) (JSM-6360). Dielectric measurements on the poled samples were carried out at 1 MHz, data was collected using a HP4284 Impedance Analyzer interfaced to a computer. The resistivity was tested by HP4339A-HP16339A. Ferroelectric hysteresis loops were tested using TF Analyzer 2000 and magnetic hysteresis loops were measured by LakeShore 7307 vibrating sample magnetometer (VSM).

3. Results and discussion

Fig. 1 shows the XRD patterns for $0.7BiFeO_3$–$0.3BaTiO_3$–x wt.% MnO_2 ceramics with $x = 0$, 0.2, 0.3, and 0.5, respectively. All ceramic samples show single perovskite structures. It is believed [3] that the $BiFeO_3$–$BaTiO_3$ solid solution structure is rhombohedral with $BiFeO_3$ above 67 mol%. XRD results also confirm that 0.7BF–0.3BT ($x = 0$) is rhombohedral. However, with 0.5 wt.% MnO_2 content doping, the structure of 0.7BF–0.3BT solid solution has entirely changed to a tetragonal perovskite structure.

Fig. 2 shows SEM images of 0.7BF–0.3BT–x wt.% MnO_2 for all different levels of x, respectively. All samples were sintered at 970 °C. These images were taken from fresh fracture surfaces. Fig. 2 shows that the grain size increases at first but decreases later with increasing content of Mn. The un-doped sample shows small and inhomogeneous grain size, which results in significant residual porosity. When 0.2 wt.% or 0.3 wt.% MnO_2 content was added, the grain size was increased with high density and the sintering ability of solid solution was improved accordingly. But when the content of MnO_2 is 0.5 wt.%, the grain size decreases, and the sintering ability of the solid solution is deteriorated, as illustrated in Fig. 2(d). The explanation is that when the concentration of MnO_2 is small (below 0.3 wt.%), manganese ions will enter crystal lattices substituting for Fe^{3+} or Ti^{4+}, which will lead to crystal lattice distortion, and thus improve the sintering ability of the ceramic. But when the concentration of MnO_2 is 0.5 wt.%, which may probably exceed the solubility limit of manganese ions in the solid solution, the sintering ability of the ceramic and the properties of the material are deteriorated accordingly.

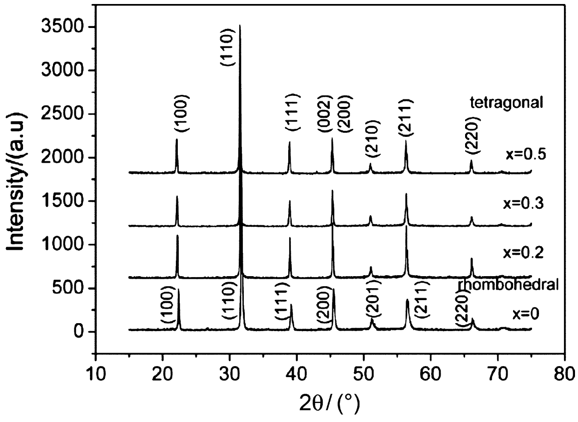

Fig. 1. XRD patterns for $0.7BiFeO_3$–$0.3BaTiO_3$–x wt.% MnO_2 solid solution system.

Fig. 3 shows the resistivity of the 0.7BF–0.3BT ceramic for different MnO_2 contents. The resistivity increases at first and then decreases with increasing content of MnO_2, which is due to the conversion of MnO_2 into Mn_2O_3 and Mn_3O_4 when at 650 and 980 °C, respectively [7]. All samples were sintered at 960–990 °C, therefore, the manganese ions are mostly in form of Mn^{3+}, but there is a reaction between Mn^{3+} and Fe^{2+}: $Mn^{3+} + Fe^{2+} \rightarrow Fe^{3+} + Mn^{2+}$, which can effectively restrain the conversion of $Fe^{3+} \rightarrow Fe^{2+}$, lowering the oxygen vacancy concentration and subsequently lowering the conductivity. Though there are Mn^{2+} and Mn^{3+} ions simultaneously in the solid solution, the amount of these ions is small, and plays little part on the electric conductivity [8]. Hence the resistivity increases evidently when the content of MnO_2 is 0.2 wt.%, namely the resistivity is $\sim 10^{13}$ Ω cm, which is the first report of high resistivity in $BiFeO_3$-based ceramics. But when the content of MnO_2 increases, the oxygen vacancies will increase due to substitution by manganese ions, since there are more Mn^{2+} ions in the vicinity of the Fe^{3+} for the reaction between Mn^{3+} and Fe^{2+}. Fe^{3+} ions will be substituted mostly by Mn^{2+} ions, but for substitution by Mn^{3+} ions cannot be excluded. Therefore, when Mn^{2+} ions substitute for Fe^{3+} or Mn^{3+} ions substitute for Ti^{4+}, oxygen vacancies will be created. Hence when the content of MnO_2 is above 0.2 wt.%, the resistivity decreases due to more oxygen vacancies, as illustrated in Fig. 3.

Fig. 4 shows dielectric constant and loss as a function of temperature for 0.7BF–0.3BT ceramic with different MnO_2 contents. Results show that the Curie temperature increases with increasing content of MnO_2, but the T_c value of all the doped samples are lower than that of the un-doped. The T_c of $BiMnO_3$ is known to be 105 K [9], and the magnitude of the melting point can be used to indicate the intensity of the ion bond, the melting points of Mn_3O_4 and TiO_2 are 1564 and 1840 °C, respectively. Hence the intensity of Mn–O bond is lower than that of Ti–O bond. If Mn ions substitute for Ti, this will weaken the stability of ferroelectric state of the solid solution. Therefore, whether Mn ions substitute for Ti or for Fe ions, the Curie temperatures of the doped samples are lower than that of the un-doped. However, with increasing MnO_2 content, the number of Mn ions entering crystal lattices increases, which will produce an interior bias electric field [10], restraining domain movement and making fully poled samples difficult to achieve. Hence the T_c will shift towards higher temperature. The dielectric loss of the un-doped sample is higher than those of the doped samples, due to the leakage conductivity of the un-doped sample being larger than those of the doped samples.

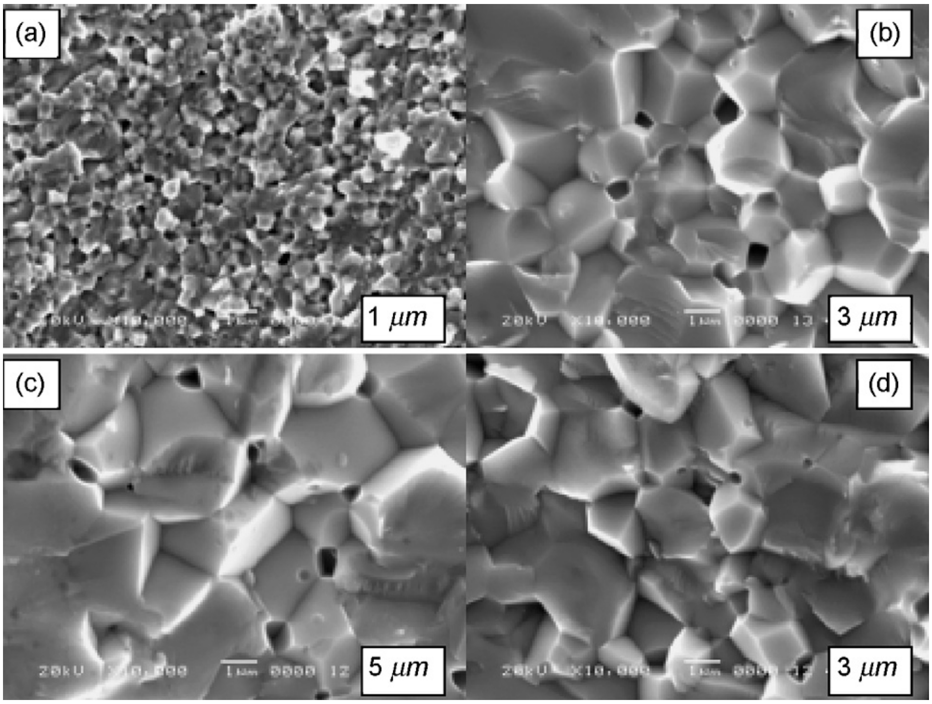

Fig. 2. SEM patterns for 0.7BiFeO$_3$–0.3BaTiO$_3$–x wt.% MnO$_2$ solid solution system. (a) $x = 0$, (b) $x = 0.2$, (c) $x = 0.3$, and (d) $x = 0.5$.

Fig. 5 shows the P–E hysteresis curves of 0.7BiFeO$_3$–0.3BaTiO$_3$–x wt.% MnO$_2$ ceramics at room temperature. Measurements were performed at a frequency of 1 Hz. Fig. 5 indicates that all samples exhibit evident ferroelectricity. The coercive electric field decreases at first and then increases with increasing content of MnO$_2$. Fig. 5(a)–(d) shows that the coercive electric fields of all samples at $x = 0$, 0.2, 0.3, and 0.5 wt.% MnO$_2$ are 3178, 2169, 2387, and 2541 V/mm, respectively. Because the sintering ability of the un-doped sample is poor and the grain size is inhomogeneous, which is not beneficial for domains reversal, the coercive field is higher. When the concentration of MnO$_2$ is 0.2 wt.%, the sintering property of ceramic can be improved and the grain size is homogeneous, which is beneficial for domains reversal,

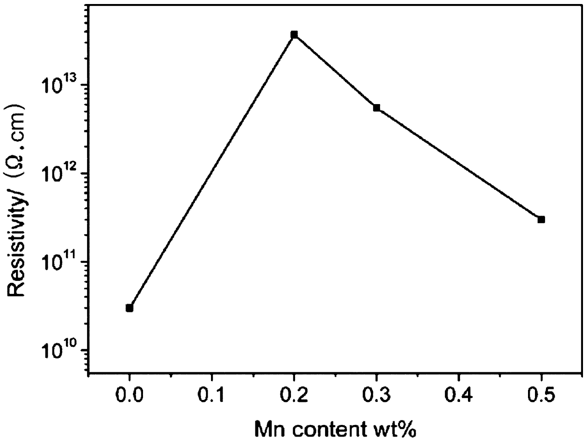

Fig. 3. Resistivity for 0.7BiFeO$_3$–0.3BaTiO$_3$–x wt.% MnO$_2$ solid solution system.

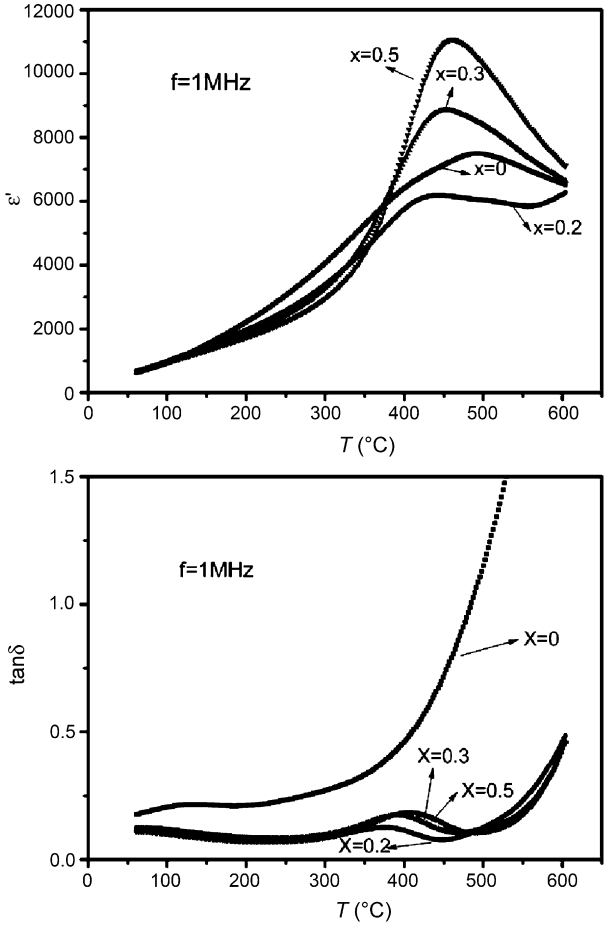

Fig. 4. Dielectric constant and dielectric loss as a function of temperature for 0.7BiFeO$_3$–0.3BaTiO$_3$–x wt.% MnO$_2$ solid solution system.

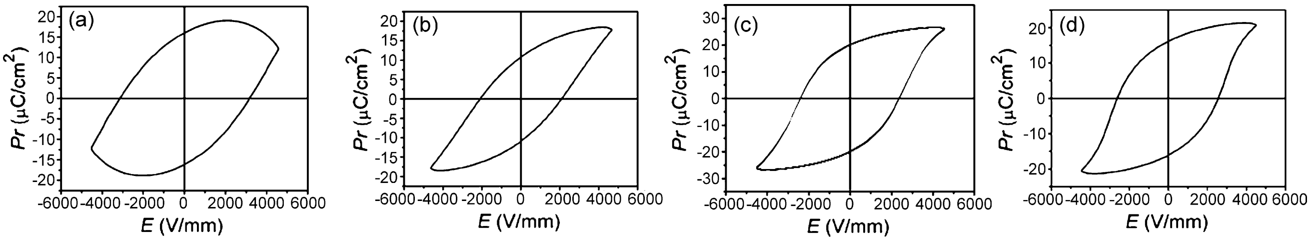

(a) 0 wt% MnO_2 Ec = 3.178 kV/mm

(b) 0.2 wt% MnO Ec = 2.169 kV/mm

(c) 0.3 wt% MnO_2 Ec = 2.387 kV/mm

(d) 0.5 wt% MnO_2 Ec = 2.541 kV/mm

Fig. 5. Ferroelectric *P*–*E* loops for $0.7BiFeO_3$–$0.3BaTiO_3$–*x* wt.% MnO_2 solid solution system.

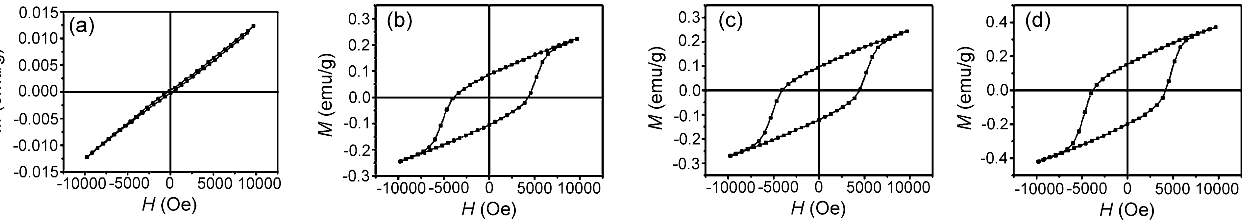

(a) 0 wt% MnO_2

(b) 0.2 wt% MnO Mr = 0.085 emu/g Hc = 4883 Oe

(c) 0.3 wt% MnO_2 Mr = 0.1 emu/g Hc = 4543 Oe

(d) 0.5 wt% MnO_2 Mr = 0.15 emu/g Hc = 4187 Oe

Fig. 6. Hysteresis loops for $0.7BiFeO_3$–$0.3BaTiO_3$–*x* wt.% MnO_2 solid solution system.

therefore the coercive field is lower. However, with further increase in the content of MnO_2, the coercive electric field will increase because MnO_2 is a "hard" dopant [10], namely when Mn^{2+} ions substitute for Fe^{3+} or Mn^{3+} ions substitute for Ti^{4+}, oxygen vacancies will be created. The appearance of the oxygen vacancies will lead to oxygen octahedral distortion, which will result in a pinning effect on domains reversal. Therefore, the coercive field increases making the materials "hard". In addition, Fig. 5(a) shows that the loop is round, which indicates significant conductive losses in the un-doped sample. Fig. 5(b)–(d) shows that *P*–*E* loops can attain saturation indicating that the doped specimens can be poled fully, which indicates that MnO_2 can decrease the conductive losses sufficiently. The structure of the specimen for $x = 0.3$ is in the morphotropic phase boundary (MPB), which will provide better polarization properties. Fig. 5(c) shows the remanent polarization P_r is 20 $\mu C/cm^2$, which is the best in all (Fig. 5(a)–(d)).

Fig. 6 shows *M*–*H* curves of $0.7BiFeO_3$–$0.3BaTiO_3$–*x* wt.% MnO_2 ceramics, measured at room temperature. Results show that the remanent magnetization M_r increases and the coercive magnetic field decreases with increasing content of Mn. For example, Fig. 6(a) shows that the sample seems paramagnetic at room temperature. But in Fig. 6(b)–(d), the M_r of the samples with 0.2, 0.3, and 0.5 wt.% MnO_2 are 0.085, 0.1, and 0.15 emu/g, respectively, and the H_c of those samples are 4883, 4543, and 4187 Oe, respectively. This can be explained in the following. On the first hand, it has been reported that the superstructure of pure $BiFeO_3$ with increasing concentration of $Pb(Fe_{0.5}Nb_{0.5})O_3$ disappears along with the spontaneous magnetic moment. It indicates that the weak ferromagnetism is more dependent on structural distortions. As the structure becomes more and more symmetrical, the spontaneous moment disappears [11]. In this investigation, when Mn^{3+} substitutes for Fe^{3+} or Ti^{4+}, the Jahn–Teller effect occurs [10]. Namely when Mn^{3+} ions enter an oxygen octahedron, the lattice around the Mn^{3+} will appear distorted, reducing the symmetry of the crystal. Therefore, the remanent magnetization of samples increases with increasing concentration of Mn. On the other hand, Gehring [12] suggested that statistical distribution of Fe^{3+} and Ti^{4+} ions in the octahedral spaces or the creation of lattice defects might lead to bulk magnetization and ferromagnetism. The Mn^{3+} can enter the crystal lattices substituting for Fe^{3+} or Ti^{4+}, which will lead to the creation of lattice defects. Hence the remanent magnetization increases with Mn content increasing. The coercive magnetic field decreases because there are always some "reverse magnetization nuclei" around the dopant in the magnetic material, and these "reverse magnetization nuclei" will develop becoming "reverse magnetization domains" under the strong enough reverse magnetization field, which will facilitate domains displacement during resisting magnetization. In turn, resistance to magnetization will be realized by domains displacement. As a result, the "reverse magnetization nuclei" will be less difficult to form if there are more lattice defects [13]. Therefore, the coercive magnetic field decreases with increasing content of MnO_2.

4. Conclusions

(1) Binary solid solutions $0.7BiFeO_3$–$0.3BaTiO_3$–*x* wt.% MnO_2 ($x = 0$, 0.2, 0.3, and 0.5) were prepared by a traditional ceramic process. The phase structure of the $0.7BiFeO_3$–$0.3BaTiO_3$ solid solution changes from rhombohedral into tetragonal phase when the content of MnO_2 is above 0.3 wt.%.

(2) When the content of MnO_2 is below 0.3 wt.%, the sintering ability of the ceramic is improved. When the content of MnO_2 is above 0.3 wt.%, the sintering ability is reduced. The Curie temperature decreases at first and then increases with increasing content of MnO_2.

(3) All ceramics samples exhibit ferroelectricity and ferromagnetism simultaneously. The insulation resistance of the material is raised sufficiently by the introduction of the manganese, and thus the doped samples can be poled fully. Ferroelectric properties have been improved greatly. With increasing content of MnO_2, the remanent magnetization M_r increases and the coercive magnetic field decreases, whereas the coercive electric field decreases at first and then increases.

Acknowledgments

This work was supported by the National Science Foundation of China (Grant Nos. 10474077 and 50632030) and Ministry of Science and Technology of China through 973-project (Grant No. 2002CB613307).

References

[1] M. Mahesh Kumar, V.R. Palkar, K. Srinivas, Ferroelectricity in a pure $BiFeO_3$ ceramic, Appl. Phys. Lett. 76 (2000) 2764–2766.

[2] J.R. Cheng, N. Li, L. Eric Cross, Structural and dielectric properties of Ga-modified $BiFeO_3$–$PbTiO_3$ crystalline solutions, J. Appl. Phys. 94 (2003) 5153–5157.

[3] M.M. Kumar, A. Srinivas, S.V. Suryanarayana, Structure property relations in $BiFeO_3$/$BaTiO_3$ solid solutions, J. Appl. Phys. 87 (2000) 855–861.

[4] T.L. Ivanova, V.V. Gagulin, Dielectric properties in the microwave range of solid solutions in the $BiFeO_3$–$SrTiO_3$ system, Ferroelectrics 265 (2002) 241–246.

[5] V.L. Mathe, K.K. Patankar, R.N. Patila, et al., Synthesis and dielectric properties of $Bi_{1-x}Nd_xFeO_3$ perovskite, J. Magn. Magn. Mater. 270 (2004) 380–388.

[6] J.S. Kim, Y.N. Choi, P.W. Jang, et al., Ferroelectric and ferromagnetic properties of $BiFeO_3$–$PrFeO_3$–$PbTiO_3$ solid solutions, J. Appl. Phys. 93 (2003) 9263–9270.

[7] F.M. Zhang, Thermal analysis of ceramics dopant-MnO_2, FeO, LiO, Piezoelect. and Acoustoopt. 20 (1998) 358–360 (in Chinese).

[8] Y.J. Huang, Magnetic Materials, Electric Industries Press, Beijing, 1994, pp. 40 (in Chinese).

[9] A. Moreira dos Santos, A.K. Cheetham, Orbital ordering as the determinant for ferromagnetism in biferroic $BiMnO_3$, Phys. Rev. B 66 (2002) 064425.

[10] W.L. Zhong, Physics of Ferroelectrics, Science Press, Bejing, 2000, pp. 430–433 (in Chinese).

[11] M.M. Kumar, S. Srinath, G.S. Kumar, et al., Spontaneous magnetic moment in $BiFeO_3$–$BaTiO_3$ solid solutions at low temperatures, J. Magn. Magn. Mater. 188 (1998) 203–212.

[12] G.A. Gehring, On the microscopic theory of the magnetoelectric effect, Ferroelectrics 161 (1994) 275–285.

[13] S.T. Jiang, W. Li, Magnetic Physics of Condensed Matter, Science Press, Bejing, 2003, pp. 353 (in Chinese).